11516 *Inorg. Chem.* **2010**, *49*, 11516–11524
DOI: 10.1021/ic1015274

Inorganic Chemistry
Article

A "Push−Pull" Mechanism for Heterolytic O−O Bond Cleavage in Hydroperoxo Manganese Porphyrins

Ning Jin, Dorothée E. Lahaye, and John T. Groves*

Department of Chemistry, Princeton University, Princeton, New Jersey 08544, United States

Received July 29, 2010

A water-soluble manganese porphyrin, 5,10,15,20-tetrakis-(1,3-dimethylimidazolium-2-yl)porphyrinatomanganese-(III) (Mn^{III}TDMImP) is shown to react with H_2O_2 to generate a relatively stable dioxomanganese(V) porphyrin complex (a compound I analog). Stopped-flow kinetic studies revealed Michaelis Menton-type saturation kinetics for H_2O_2. The visible spectrum of a compound 0 type intermediate, assigned as Mn^{III}(OH)(OOH)TDMImP, can be directly observed under saturating H_2O_2 conditions (Soret band at 428 nm and Q bands at 545 and 578 nm). The rate-determining O−O heterolysis step was found to have a very small activation enthalpy ($\Delta H^{\neq}$ = 4.2 ± 0.2 kcal mol^{-1}) and a large, negative activation entropy ($\Delta S^{\neq}$ = −36 ± 1 cal mol^{-1} K^{-1}). The O−O bond cleavage reaction was pH independent at 8.8 < pH < 10.4 with a first-order rate constant of 66 ± 12 s^{-1}. These observations indicate that the O−O bond in Mn^{III}(OH)(OOH)TDMImP is cleaved via a concerted "push−pull" mechanism. In the transition state, the axial (proximal) $^{-}$OH is partially deprotonated ("push"), while the terminal oxygen in $^{-}$OOH is partially protonated ("pull") as a water molecule is released to the medium. This mechanism is reminiscent of O−O bond cleavage in heme enzymes, such as peroxidases and cytochrome P450, and similar to the fast, reversible O−Br bond breaking and forming reaction mediated by similar manganese porphyrins. The small enthalpy of activation suggests that this O−O bond cleavage could also be made reversible.

Introduction

Heme oxygenases, such as cytochrome P450, cytochrome c oxidase, peroxidases and catalases, carry out important biological redox processes using hydrogen peroxide and molecular dioxygen. A crucial step in the catalytic cycle of these enzymes is the heterolytic cleavage of the O−O bond in an iron−hydroperoxo species [Fe^{III}−OOH, compound (cpd) 0] generating the active oxidizing species [an oxoFe^{IV} porphyrin radical cation, compound (cpd) I].[1−6] Inefficient cleavage causes wasteful loss of hydrogen peroxide called "uncoupling". In native enzymes, facile and ensured heterolysis of the O−O bond is proposed to be achieved by sophisticated machinery of proximal and distal amino acids known as the "push−pull" effect.[7] Specifically, axial ligands, such as histidine or cysteine, provide electron density to the antibonding O−O orbital through the iron center (the "push"), while the polar residues in distal pocket regulate proton delivery to the terminal oxygen creating a better leaving group (the "pull"). The push−pull effect has been extensively studied on cytochrome P450,[8] peroxidases,[9] catalase,[10] reengineered myoglobin,[11] and heme model systems.[12,13]

Despite the extensive understanding of the mechanism of heme oxygenases, direct observation of the O−O bond cleavage in enzymes has been difficult due to complex catalytic cycles and short-lived intermediates. For example, cpd I species for cytochrome P450 have been particularly elusive and controversial,[14,15] while cryogenic conditions are required for the observation of cpd 0 species of P450, chloroperoxidase, and horseradish peroxidase.[16−19]

*Corresponding author. E-mail: jtgroves@princeton.edu. Telephone: (609) 258-3593.

(1) Shaik, S.; Cohen, S.; Wang, Y.; Chen, H.; Kumar, D.; Thiel, W. *Chem. Rev*. **2010**, *110*, 949–1017.
(2) Groves, J. T. In *Cytochrome P450: Structure, Mechanism, and Biochemistry*; 3rd ed.; Ortiz de Montellano, P. R., Ed.; Kluwer Academic/Plenum: New York, 2005, p 1−44.
(3) Denisov, I. G.; Makris, T. M.; Sligar, S. G.; Schlichting, I. *Chem. Rev*. **2005**, *105*, 2253–2277.
(4) Meunier, B.; de Visser, S. P.; Shaik, S. *Chem. Rev*. **2004**, *104*, 3947–3980.
(5) Ortiz de Montellano, P. R. *Chem. Rev*. **2010**, *110*, 932–948.
(6) Guengerich, F. P. *Chem. Res. Toxicol*. **2008**, *21*, 70–83.
(7) Dawson, J. H. *Science* **1988**, *240*, 433–439.
(8) Sono, M.; Roach, M. P.; Coulter, E. D.; Dawson, J. H. *Chem. Rev*. **1996**, *96*, 2841–2887.
(9) Derat, E.; Shaik, S. *J. Phys. Chem. B* **2006**, *110*, 10526–10533.
(10) Fita, I.; Rossmann, M. G. *J. Mol. Biol*. **1985**, *185*, 21–37.
(11) Ozaki, S. I.; Roach, M. P.; Matsui, T.; Watanabe, Y. *Acc. Chem. Res*. **2001**, *34*, 818–825.
(12) Groves, J. T.; Watanabe, Y. *J. Am. Chem. Soc*. **1988**, *110*, 8443–8452.
(13) Watanabe, Y. In *The Porphyrin Handbook*; Kadish, K. M., Smith, K. M., Guilard, R., Eds.; Academic Press: San Diego, CA, 2000; Vol. *4*, p 97−118.
(14) Rittle, J.; Younker, J. M.; Green, M. T. *Inorg. Chem*. **2010**, *49*, 3610–3617.
(15) Newcomb, M.; Halgrimson, J. A.; Horner, J. H.; Wasinger, E. C.; Chen, L. X.; Sligar, S. G. *Proc. Natl. Acad. Sci. U.S.A*. **2008**, *105*, 8179–8184.

 Published on Web 11/16/2010

Studies of synthetic metalloporphyrins[2] and related porphyrinoid complexes[20−22] provide mechanistic insights to the chemistry of iron−oxo and the iron−peroxo intermediates in heme enzymes and hold potential for efficient oxidative catalysts.[23] In the biomimetic systems, the structure−reactivity pattern can be fine-tuned, and the active intermediates well characterized in some cases. For example, Naruta et al.[24−27] and Tajima et al.[28] have characterized hydroperoxoiron(III) porphyrin complexes at low temperatures, and a model heme−peroxocopper complex has been described by Karlin et al.[29] Composite rate constants for peroxide coordination and O−O bond cleavage by synthetic iron porphyrins have been determined by van Eldik et al.[30,31] Nocera et al. demonstrated that O−O bond homolysis is efficiently inhibited by a single poised carboxylic acid group over an iron redox center in a model porphyrin system.[32] Various reaction channels for Fe^{III}−O−OH have been extensively investigated by computational methods.[1,33−35]

Manganese reconstituted heme enzymes have been studied in anticipation that high-valent manganese oxo species are more stable than their iron counterparts. However, in a protein environment the Mn^{V}=O heme entity has not been observed in horseradish peroxidase,[36] cytochrome P450 CYP101,[37] or microperoxidase.[38] Instead, Mn^{IV}=O species coupled with a protein radical were identified in these systems. Nonetheless, manganese-mediated O−O bond-breaking and -forming reactions are particularly important in regard to artificial photosynthetic systems.[39] For example, nucleophilic attack of hydroxide ion on a Mn^{V}=O moiety has been suggested for the critical O−O bond-forming step in the photosynthetic water oxidation process.[40] A bridged Mn^{V} porphyrin dimer has been demonstrated to oxidize water into dioxygen,[41] and recently reversible O−O bond cleavage was observed for a manganese corrole system.[42]

Recently, we described a series of *trans*-dioxomanganese(V) porphyrin complexes,[43] which are functional analogs of cpd I.[44,45] We have also described a model oxoiron(IV) porphyrin cation radical with very high reactivity toward C−H bond hydroxylation that derives from an iron peroxo precursor.[12,46] In the present work, we report a kinetic study of the reaction between H_2O_2 and an electron-deficient water-soluble manganese porphyrin to generate a dioxoMn^{V} species in aqueous solution. These studies have allowed direct measurements of the manganese-mediated, heterolytic O−O bond-cleavage step.

Results

Manganese(III)-5,10,15,20-tetrakis-(1,3-dimethylimidazolium-2-yl)porphyrin chloride (Mn^{III}TDMImP, **1**) can be oxidized with peroxides or hypohalites to generate the quasistable Mn^{V} and Mn^{IV} porphyrins. The reaction is initialized by binding of the oxidant to the Mn^{III} center, producing a cpd 0 like species (Mn^{III}−OOH or Mn^{III}−OX). Heterolytic breaking of the O−O or O−X bond yields the cpd I type Mn^{V}=O porphyrin species, while a homolytic cleavage gives the cpd II type Mn^{IV}=O porphyrin species (Scheme 1). Analogous to the iron system, the choice between one and two electron oxidation pathways is heavily dependent on the oxidant used.[47−50] Correspondingly, for **1** in aqueous solution, dioxoMn^{V}TDMImP (**2**) is formed by oxidants, such as HSO_5^-, *m*-chloroperoxybenzoic acid (*m*-CPBA), H_2O_2, ClO, or BrO, and Mn^{IV}TDMImP (**3**) is produced by *t*-BuOOH, cumene hydroperoxide, or ONOO. The characteristic ^{1}H NMR spectrum for diamagnetic **2** and X-band electron paramagnetic resonance (EPR) spectrum for high-spin, $S = 3/2$ **3** are shown in the Supporting Information.

The two aqua ligands in $Mn^{III}(OH_2)_2$TDMImP (**1**) can be successively deprotonated forming first a hydroxo-aqua and then a dihydroxo complex. Spectroscopic titration gives $pK_{a1} = 7.8 \pm 0.2$ and $pK_{a2} = 8.8 \pm 0.2$. Similarly, pK_a for Mn^{IV}(O)(OH_2)TDMImP (**3**) was measured to be 9.4 ± 0.4.

(16) Schlichting, I.; Berendzen, J.; Chu, K.; Stock, A. M.; Maves, S. A.; Benson, D. E.; Sweet, B. M.; Ringe, D.; Petsko, G. A.; Sligar, S. G. *Science* **2000**, *287*, 1615–1622.
(17) Davydov, R.; Makris, T. M.; Kofman, V.; Werst, D. E.; Sligar, S. G.; Hoffman, B. M. *J. Am. Chem. Soc.* **2001**, *123*, 1403–1415.
(18) Baek, H. K.; Vanwart, H. E. *Biochemistry* **1989**, *28*, 5714–5719.
(19) Denisov, I. G.; Dawson, J. H.; Hager, L. P.; Sligar, S. G. *Biochem. Biophys. Res. Commun.* **2007**, *363*, 954–958.
(20) Gross, Z.; Gray, H. B. *Adv. Synth. Catal.* **2004**, *346*, 165–170.
(21) Kerber, W. D.; Goldberg, D. P. *J. Inorg. Biochem.* **2006**, *100*, 838–857.
(22) Prokop, K. A.; Visser, S. P. d.; Goldberg, D. P. *Angew. Chem., Int. Ed.* **2010**, *49*, ASAP.
(23) Meunier, B., Robert, A., Pratviel, G., Bernadou, J. In *The Porphyrin Handbook*; Kadish, K. M., Smith, K. M., Guilard, R., Ed.; Academic Press: San Diego, 2000; Vol. *4*, p 119−187.
(24) Liu, J. G.; Shimizu, Y.; Ohta, T.; Naruta, Y. *J. Am. Chem. Soc.* **2010**, *132*, 3672–3673.
(25) Liu, J. G.; Ohta, T.; Yamaguchi, S.; Ogura, T.; Sakamoto, S.; Maeda, Y.; Naruta, Y. *Angew. Chem., Int. Ed.* **2009**, *48*, 9262–9267.
(26) de Visser, S. P.; Valentine, J. S.; Nam, W. *Angew. Chem., Int. Ed.* **2010**, *49*, 2099–2101.
(27) Karlin, K. D. *Nature* **2010**, *463*, 168–169.
(28) Tajima, K.; Oka, S.; Edo, T.; Miyake, S.; Mano, H.; Mukai, K.; Sakurai, H.; Ishizu, K. *J. Chem. Soc., Chem. Commun.* **1995**, 1507–1508.
(29) Ghiladi, R. A.; Chufan, E. E.; del Rio, D.; Solomon, E. I.; Krebs, C.; Huynh, B. H.; Huang, H. W.; Moenne-Loccoz, P.; Kaderli, S.; Honecker, M.; Zuberbuhler, A. D.; Marzilli, L.; Cotter, R. J.; Karlin, K. D. *Inorg. Chem.* **2007**, *46*, 3889–3902.
(30) Fertinger, C.; Hessenauer-Ilicheva, N.; Franke, A.; van Eldik, R. *Chem.—Eur. J.* **2009**, *15*, 13435–13440.
(31) Brausam, A.; Eigler, S.; Jux, N.; van Eldik, R. *Inorg. Chem.* **2009**, *48*, 7667–7678.
(32) Soper, J. D.; Kryatov, S. V.; Rybak-Akimova, E. V.; Nocera, D. G. *J. Am. Chem. Soc.* **2007**, *129*, 5069–5075.
(33) Altarsha, M.; Benighaus, T.; Kumar, D.; Thiel, W. *J. Biol. Inorg. Chem.* **2010**, *15*, 361–372.
(34) Shaik, S.; Kumar, D.; de Visser, S. P.; Altun, A.; Thiel, W. *Chem. Rev.* **2005**, *105*, 2279–2328.
(35) Surawatanawong, P.; Tye, J. W.; Hall, M. B. *Inorg. Chem.* **2010**, *49*, 188–198.
(36) Nick, R. J.; Ray, G. B.; Fish, K. M.; Spiro, T. G.; Groves, J. T. *J. Am. Chem. Soc.* **1991**, *113*, 1838–1840.
(37) Makris, T. M.; von Koenig, K.; Schlichting, I.; Sligar, S. G. *J. Inorg. Biochem.* **2006**, *100*, 507–518.
(38) Veeger, C. *J. Inorg. Biochem.* **2002**, *91*, 35–45.
(39) McEvoy, J. P.; Brudvig, G. W. *Chem. Rev.* **2006**, *106*, 4455–4483.
(40) Betley, T. A.; Wu, Q.; Van Voorhis, T.; Nocera, D. G. *Inorg. Chem.* **2008**, *47*, 1849–1861.
(41) Shimazaki, Y.; Nagano, T.; Takesue, H.; Ye, B. H.; Tani, F.; Naruta, Y. *Angew. Chem., Int. Ed.* **2004**, *43*, 98–100.
(42) Kim, S. H.; Park, H.; Seo, M. S.; Kubo, M.; Ogura, T.; Klajn, J.; Gryko, D. T.; Valentine, J. S.; Nam, W. *J. Am. Chem. Soc.* **2010**, *132*, 14030–14032.
(43) Jin, N.; Ibrahim, M.; Spiro, T. G.; Groves, J. T. *J. Am. Chem. Soc.* **2007**, *129*, 12416–12417.
(44) Jin, N.; Groves, J. T. *J. Am. Chem. Soc.* **1999**, *121*, 2923–2924.
(45) Jin, N.; Bourassa, J. L.; Tizio, S. C.; Groves, J. T. *Angew. Chem., Int. Ed.* **2000**, *39*, 3849–3851.
(46) Bell, S. R.; Groves, J. T. *J. Am. Chem. Soc.* **2009**, *131*, 9640–9641.
(47) Nam, W.; Choi, H. J.; Han, H. J.; Cho, S. H.; Lee, H. J.; Han, S. Y. *Chem. Commun.* **1999**, 387–388.
(48) Almarsson, O.; Bruice, T. C. *J. Am. Chem. Soc.* **1995**, *117*, 4533–4544.
(49) Groves, J. T.; Watanabe, Y. *Inorg. Chem.* **1986**, *25*, 4808–4810.
(50) Lee, J. B.; Hunt, J. A.; Groves, J. T. *J. Am. Chem. Soc.* **1998**, *120*, 6053–6061.

Scheme 1

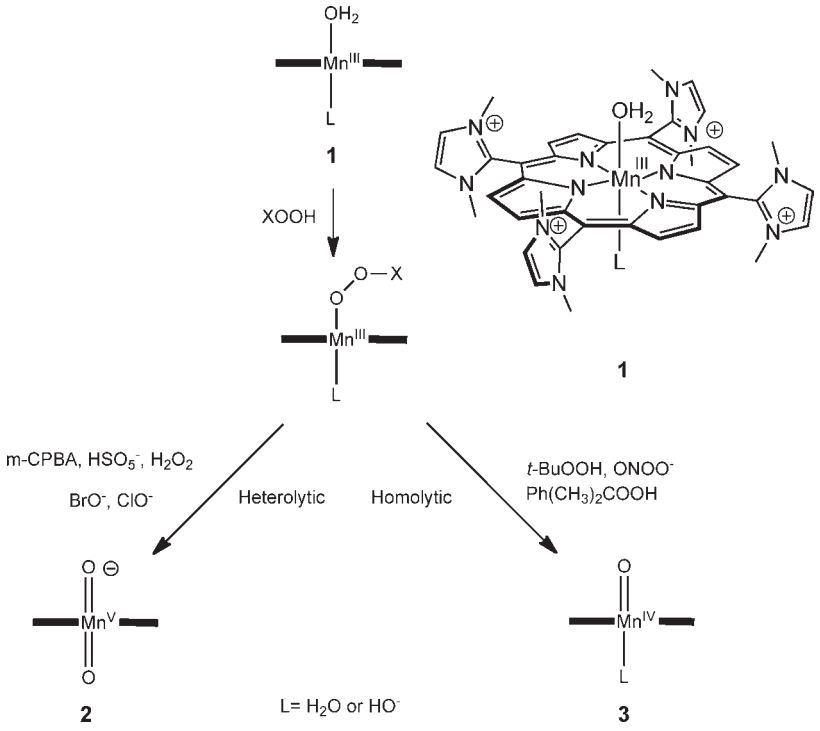

Table 1. UV−vis Absorbances λ_{max} (nm) and ε ($M^{-1}cm^{-1}$) for MnTDMImP in Aqueous Solution[a]

complexes	Soret band (log ε)	Q-band (log ε)
$Mn^{III}(OH_2)_2$	446(5.07), 348(4.69)	553(4.03), 587(3.89)
$Mn^{III}(OH)_2$	435(5.16), 336(4.55)	559(4.23), 591(3.93)
$Mn^{IV}(O)(OH_2)$	422(4.93)	545(4.10), 578(4.11)
$Mn^{IV}(O)(OH)$	437(4.92)	551(4.17), 582(4.01)
$Mn^{V}(O)_2$	426(5.18), 336(4.64)	544(4.23), 578(4.08)

[a] See full spectra in Supporting Information

For Mn^{V}TDMImP (**2**), the *trans*-dioxo nature of this complex was confirmed by resonance Raman studies in alkaline conditions.[43] The self-decay of the Mn^{V} porphyrin species is accelerated in acidic conditions. In stopped-flow pH-jump experiments we did not observe the protonated form (the oxo-hydroxo or oxo-aqua Mn^{V} species) for a pH as low as 4.3 at room temperature. Thus, we conclude that **2** remains as a dioxo complex throughout this study. UV−vis spectra for **1**−**3** are summarized in Table 1.

In the context of O−O bond-breaking and -forming reactions, we thoroughly investigated the H_2O_2 oxidation of **1**. In stopped-flow kinetic studies, buffered aqueous solutions containing **1** (2−20 μM) were rapidly mixed with H_2O_2, and generation of **2** was followed spectroscopically. The homolytic product **3** was not observed upon close scrutiny of the reaction spectra under different pH and H_2O_2 concentrations, probably due to the very high-thermodynamic barrier of producing ·OH. There is no significant reaction between **2**, **3** (generated independently), and excess H_2O_2 under our reaction conditions, although a very large excess of H_2O_2 does "bleach" the porphyrin chromophore. Comproportionation and disproportionation reactions between **1**−**3** were also not observed under these conditions.[51]

(51) Zhang, R.; Horner, J. H.; Newcomb, M. *J. Am. Chem. Soc.* **2005**, *127*, 6573–6582.

The *trans*-dioxoMn^{V} species **2** has a lifetime of several minutes in alkaline conditions. We noticed that the H_2O_2 oxidation reaction is significantly slowed at either mildly acidic (pH < 7) or very alkaline (pH > 13) conditions with an optimal reaction window of 8.5 < pH < 11.5.

Figure 1 shows time-resolved UV−vis spectra changes for this reaction at pH 9.66; at low concentration of H_2O_2 (0.25 mM), the transformation of **1** to **2** has clear isosbestic points at 430, 552, 572, and 587 nm (Figure 1a). Upon addition of a large excess of H_2O_2 (25 mM), a new species **4** was instantly formed (Figure 1b) and then converted to **2**; the corresponding isosbestic points were shifted to 432, 554, 571, and 584 nm. The intermediate **4** is not completely generated at low-concentration H_2O_2 (< 5 mM). If fully formed, spectrum of **4** (Soret band at 428 nm and Q-band at 545 and 578 nm) can be deconvoluted from time-resolved spectra changes by SPECTFIT/32 software using an A → B → X model (Figure 2a). The concentration for **4** could be followed readily by its distinctive Soret shoulder at 382 nm, where its absorbance is higher than both **1** and **2** (Figure 1b inset). UV−vis spectra of the reaction solution right after mixing (1−3 ms and 2 ms diode array integration time) are shown in Figure 2b. When the H_2O_2 concentration is increased from 0.25 to 25 mM, the tight isosbestic points suggest that the concentration of **2** is insignificant over this time period. It is evident that the ratio of **4** to **1** gradually increased and eventually saturated with increasing H_2O_2 concentrations.

The time course of the reaction of **1** to afford **2** was monitored at 426 nm, which is the λ_{max} for **2**. Also, the absorbance of **1** and **4** are very similar at this wavelength. The collected kinetic profiles could be satisfactorily fit to a single exponential equation to afford pseudofirst-order rate constants. The apparent rate constants (k_{obs}) varied linearly with the concentration of **1** at low [H_2O_2] and became saturating with a large excess of H_2O_2 (Figure 3a); k_{obs} was not dependent on

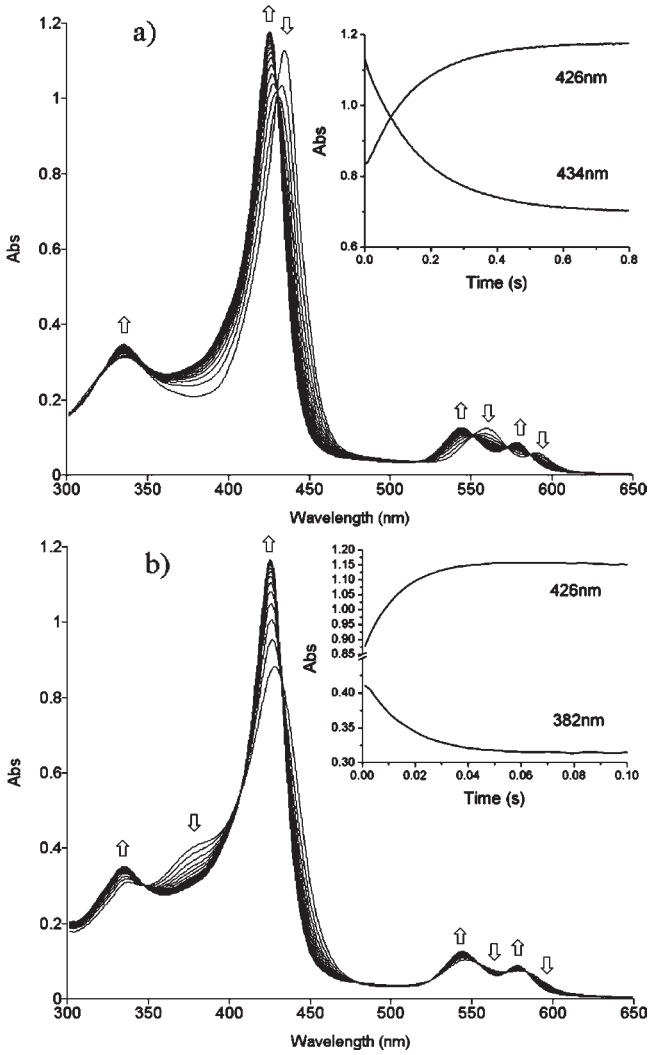

Figure 1. Time-resolved UV−vis spectra of the reaction of **1** (7.7 μM) with H_2O_2 at pH 9.66, 50 mM borate buffer. (a) At 0.25 mM H_2O_2, 200 scans in 0.8 s, 2 ms photodiode array integration time, every 10th scan is shown at 2, 42, 82, 122 ms, etc. (b) At 25 mM H_2O_2, 50 scans in 0.1s, 2 ms integration time, every 2nd scan is shown at 1, 5, 9, 13 ms, etc. Insets: Absorbance changes over time for **1** (λ_{max} = 434 nm), **2** (426 nm), and **4** (382 nm).

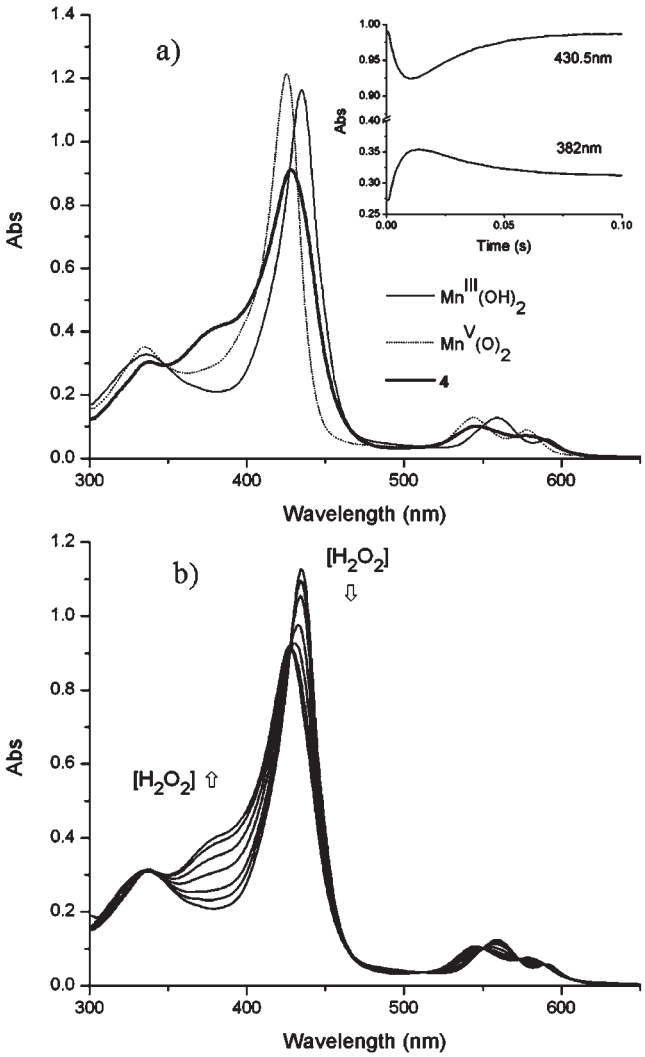

Figure 2. (a) Deconvoluted UV−vis spectra for the starting **1**, Mn^{III}−OOH intermediate **4** and oxoMn^{IV} product **3** for the reaction between 7.7 μM **1** and H_2O_2 in 50 mM pH 9.66 borate buffer. (b) UV−vis spectra snapshots at 1−3 ms after mixing (2 ms integration time) for the reaction between 7.7 μM **1** and various concentrations of H_2O_2 in 50 mM and pH 9.66 borate buffer. Plotted traces correspond to H_2O_2 concentration at 0.25, 1, 2, 4.5, 8, 15, and 25 mM, respectively. Spectra for **1** and **2** are not shown for clarity.

the total buffer concentration (20−160 mM), indicating a lack of general acid−base catalysis.

Observation of the Michaelis−Menten-type saturation kinetics suggests the mechanism of a reversible formation of intermediate **4** and the subsequent irreversible conversion of **4** to **2** (Scheme 2). At a given pH value, the observed rate pseudofirst-order constant k_{obs} can be derived as eq 1, assuming fast equilibrium between **1** and **4**.

$$k_{obs} = \frac{k_2[H_2O_2]}{[H_2O_2] + \frac{1}{K}} \quad (1)$$

In a double reciprocal form:

$$\frac{1}{k_{obs}} = \frac{1}{k_2} + \frac{1}{k_2 K}\frac{1}{[H_2O_2]} \quad (2)$$

We determined k_2 from the intercept of the double reciprocal plot of k_{obs} vs H_2O_2 concentration (eq 2 and Figure 3b) as 58 ± 12, 67 ± 6, 78 ± 5, 65 ± 3, and 63 ± 5 s^{-1} at pH 8.80, 9.01, 9.46, 9.87, and 10.43, respectively, with an average value of 66 ± 12 s^{-1}. It should be noted that **2** is not fully formed beyond the optimal reaction window, and measuring k_2 results in very large errors.

The temperature dependence of k_2 was investigated from 13 to 35 °C at pH 9.87. Activation enthalpy $\Delta H^{\neq}$ = 4.2 ± 0.2 kcal mol^{-1} and activation entropy $\Delta S^{\neq}$ = −36 ± 1 cal mol^{-1} K^{-1} were obtained (see Eyring plot in Supporting Information). A solvent kinetic isotope effect (k_{H2O}/k_{D2O}) of 2.2 ± 0.1 for k_2 was also determined at pH (pD) = 9.34 (see Supporting Information).

At low concentrations of H_2O_2, k_{obs} appeared to be linearly dependent on the H_2O_2 concentration. The apparent second-order rate constant k_{app} could be measured by the linear fitting of k_{obs} vs $[H_2O_2]$. The pH dependence of k_{app} for H_2O_2, HSO_5^-, and *t*-BuOOH is shown in Figure 4. HSO_5^- is a powerful two-electron oxidant with a good leaving group and was capable of converting Mn^{III}TDMImP to dioxo-Mn^{V} stoichiometrically. On the other hand, *t*-BuOOH oxidized

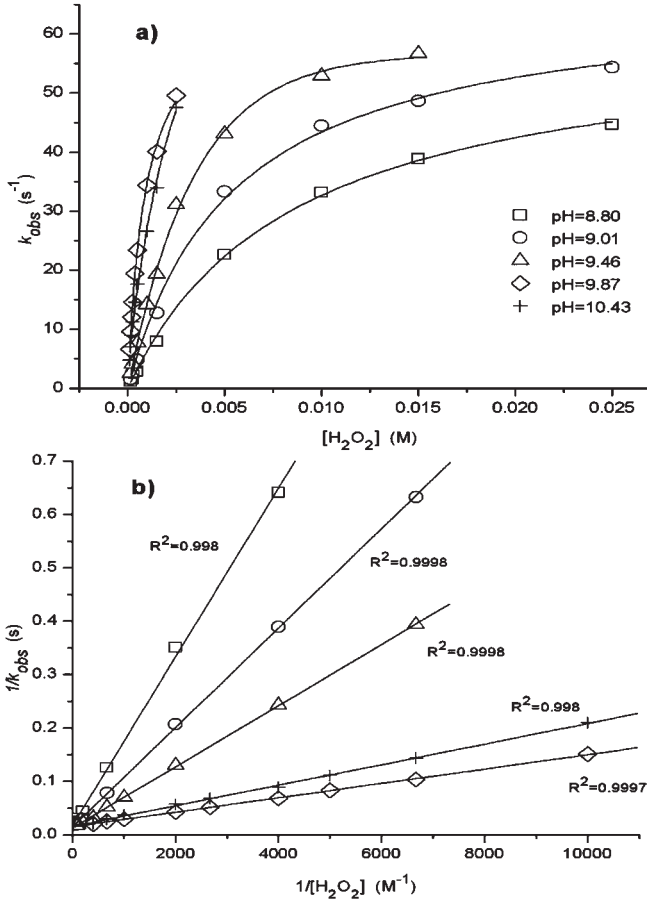

Figure 3. (a) Variations of k_{obs} as a function of H_2O_2 concentration (fitted to a hyperbolic equation) for the reaction between 5 μM **1** and H_2O_2 in 25 mM and pH 8.80, 9.01, 9.46, 9.87, and 10.43 borate (first three) or carbonate (last two) buffer (μ = 0.1 M $NaClO_4$). (b) Double reciprocal plot of the data in (a), all linear fits have similar intercepts.

Scheme 2

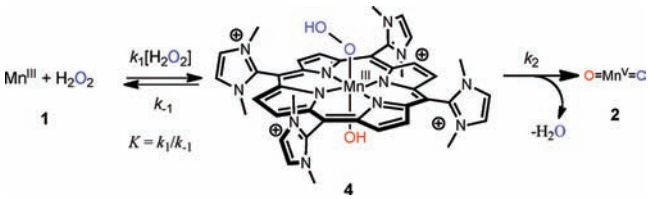

Mn^{III} to Mn^{IV} via an O−O bond homolysis mechanism. For all three oxidants, k_{app} had maximum values at pH ≈ 10.

Analogous *trans*-dioxoMn^{V} species of other water-soluble porphyrins (TM-2-PyP, TM-4-PyP, and TF_4TMAP; acronyms in the Experimental Section) could also be generated with H_2O_2. The reaction rates for these similarly charged cationic porphyrins were significantly faster than that of Mn^{III}TDMImP. For Mn^{III}TM-2-PyP, k_2 was measured to be $1.0 \pm 0.1 \times 10^3$ s^{-1} in the pH range of 9.5−10.4 (data not shown). For Mn^{III}TM-4-PyP and $Mn^{III}TF_4TMAP$, the H_2O_2 oxidation rates are too fast to observe saturation kinetics on our stopped-flow apparatus; their O−O bond cleavage rates were estimated to be at least 10^4 s^{-1}.

Discussion

Identity of the Mn^{III}/H_2O_2 Intermediate. Kinetic analysis of the reaction between Mn^{III}TDMImP and H_2O_2 showed that the intermediate **4** was rapidly generated prior to the formation of the dioxoMn^{V}TDMImP (**2**). A hydroperoxoMn^{III} species is the most plausible structure for this intermediate. The kinetic data indicated a reversible binding and dissociation of H_2O_2 to Mn^{III}TDMImP that is much faster than the subsequent O−O bond cleavage step (k_2). This is corroborated by the fact that axial aqua ligands for Mn^{III} porphyrins in aqueous solution are very labile. For example, the rate for displacement of an aqua ligand in Mn^{III}TM-4-PyP by various phosphorus ligands was measured by Summers et al. using ^{31}P NMR line-broadening techniques and ligand exchange rates ranging from 5×10^5 to 9×10^6 M^{-1} s^{-1}.[52]

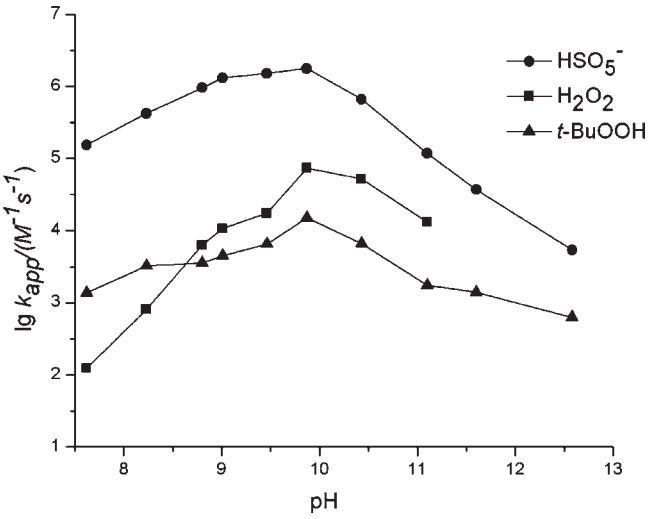

Figure 4. The pH dependence of apparent second-order rate constants k_{app} for HSO_5^- H_2O_2, and *t*-BuOOH oxidation of Mn^{III}TDMImP. Mn^{V} is generated with HSO_5^- H_2O_2, and Mn^{IV} with *t*-BuOOH.

There are several protons involved in the H_2O_2 binding process, which may influence the overall reaction rate dramatically. As can be seen in Figure 4, the apparent second-order rate constant (k_{obs}) for the overall reaction displays a bell-shaped pH profile. Despite the complicated acid−base equilibria, k_2 for the O−O bond cleavage step in **4** was found to be pH independent between pH 8.80 and 10.43, where the value can be reliably determined (Figure 3). Over this range of pH, the average value of k_2 was found to be 66 ± 12 s^{-1}. It can be determined from this result that there is no net proton gain or loss during the rate determining k_2 step.

A similar pH-independent effect for O−O bond cleavage has been observed for H_2O_2 oxidation of Fe^{III} or Mn^{III} microperoxidase-8[53] and conversion of a hydroperoxochromium(III)(tetraazamacrocycle) species to a chromium(V) complex.[54,55] For this latter case there is the additional analogy that the high-valent chromium product was formulated by Bakac et al. as a dioxo compound $[O{=}Cr^{V}{=}O]^+$, although the reactive channel could also lead to $[HO{-}Cr^{V}{=}O]^{2+}$.[54] Significantly, the O−O bond heterolysis for the hydroperoxomanganese(III) species **4** is 2.6×10^3 fold faster than that of the chromium case.

(52) Summers, J. S.; Base, K.; Boukhalfa, H.; Payne, J. E.; Shaw, B. R.; Crumbliss, A. L. *Inorg. Chem.* **2005**, *44*, 3405–3411.
(53) Primus, J. L.; Grunenwald, S.; Hagedoorn, P. L.; Albrecht-Gary, A. M.; Mandon, D.; Veeger, C. *J. Am. Chem. Soc.* **2002**, *124*, 1214–1221.
(54) Pestovsky, O.; Bakac, A. *J. Chem. Soc., Dalton Trans.* **2005**, 556–560.
(55) Song, W. J.; Bakac, A. *Inorg. Chem.* **2010**, *49*, 150–156.

Scheme 3

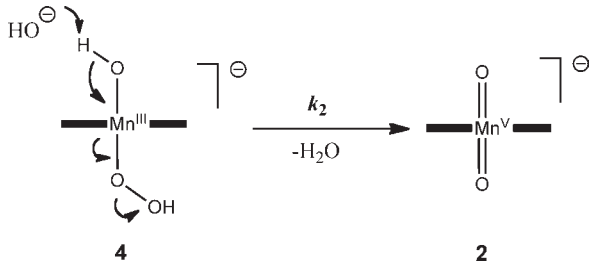

The spectroscopic titration data indicate that coordination of H_2O (pK_a = 15.7) to the manganese center in Mn^{III}TDMImP lowers its pK_a value by about 8 pH units (to a value of 7.8). A similar effect is expected for H_2O_2, based on the estimation of a similar shift of around 8 pH units for H_2O_2 upon its coordination to the ferric heme center of peroxidase (pK_a for free H_2O_2 = 11.6 and for coordinated H_2O_2 = 3.2−4).[56] It can thus be safely assumed that in **4** the coordinated H_2O_2 is deprotonated in the pH region under study. On the other hand, the better electron-withdrawing ability of HO_2^- relative to OH^- would render the aqua ligand trans to HO_2^- (pK_a = 8.8 for H_2O trans to OH^-) to be more acidic as well. Therefore, in the optimal reaction pH range, the most reasonable structure for spectroscopically observable intermediate **4** should be a hydroxo−hydroperoxo complex, i.e., Mn^{III}-(OH)(OOH)−TDMImP, as depicted in Scheme 2.

O−O Bond Heterolysis Mechanism. The conversion of Mn^{III}(OH)(OOH)−TDMImP (**4**) to the *trans*-dioxoMn^V species **2** is a significant step, since it closely resembles the cpd 0 to cpd I transformation of heme proteins. In the stoichiometric sense, **4** and **2** differ with just a molecule of water. We propose a concerted mechanism (Scheme 3) in which the O−O bond heterolysis is coupled to the deprotonation of the trans OH^- ligand, mimicking a "push−pull" mechanism found in heme enzymes. Here the relatively weak field hydroxo ligand is transformed into a terminal oxo group with a formal double bond to manganese.

A concerted, water catalyzed, mechanism is consistent with the pH insensitivity and the large negative activation entropy ($\Delta S^{\neq} = -36 \pm 1$ cal mol^{-1} K^{-1}). The unusually large negative entropy for this single molecular reaction corroborates a highly ordered transition state, contributed largely by simultaneous solvation of a proton and a hydroxide ion as well as manganese oxidation state, spin state, and bond length changes. While the spin state of the Mn^{III}−OOH intermediate **4** is uncertain, it is almost certainly paramagnetic. By contrast, the product *trans*-dioxoMn^V complex **2** is diamagnetic. Accordingly, the transformation depicted in Scheme 3 is formally spin forbidden. Spin-state crossing effects have been invoked recently by Mayer et al. to explain aspects of the kinetics observed for chromium porphyrins.[57] We note, however, that the very fast and reversible oxo transfer observed for the reaction of *trans*-dioxoMn^V porphyrins with bromide ion indicates that any spin-state crossing kinetic barrier will be very small.[45,58]

The measured entropy term for the conversion of **4** to **2** is more than double that of the enthalpy term in activation free energy $\Delta G^{\neq}$. On the other hand, the small activation enthalpy ($\Delta H^{\neq} = 4.2 \pm 0.2$ kcal mol^{-1}) is in line with a value estimated for horseradish peroxidase (4.1 kcal/mol),[59] manganese reconstituted HRP (5.5 kcal/mol),[60] and peroxyacyl Fe^{III}(TMP) (3.6 kcal/mol; $\Delta S^{\neq} \sim -25$ cal mol^{-1} K^{-1}).[12] For comparison, the formation of the O=Cr^V=O species discussed above from its hydroperoxo Cr^{III} precursor has $\Delta H^{\neq} = 12.8$ kcal mol^{-1} and $\Delta S^{\neq} = -19$ cal mol^{-1} K^{-1} in aqueous solution,[54] while homolysis in a *t*-BuO−O−Fe^{III} complex has $\Delta H^{\neq} = 12.4$ kcal mol^{-1} and $\Delta S^{\neq} = -18$ cal mol^{-1} K^{-1} in CH_3CN.[61]

The moderate kinetic isotope solvent effect (KISE) of 2.2 is expected for the solvation catalysis shown in Scheme 2, in which proton hydroxide transfer is synchronous with O−O bond cleavage. A direct proton transfer to the terminal oxygen in Mn^{III}−OOH in the transition state would be expected to produce a much larger primary isotope effect.[62]

The porphyrin ligand structure greatly influences the O−O bond cleavage rate. It has been shown that electron-rich porphyrin ligands promote O−O bond cleavage in iron porphyrin systems, simulating a "push" effect.[12] The positive charge on the imidazolium group in TDMImP is delocalized over both nitrogens and C2, providing greater proximity to the *meso*-porphyrin carbons. As a result, TDMImP exerts a stronger electron-withdrawing effect than the similarly charged TM-2-PyP, TM-4-PyP, and TF_4TMAP. Indeed, the half wave potential ($E_{1/2}$) of the Mn^{III}/Mn^{II} redox pair for TDMImP is 320 mV (vs NHE),[63] higher than that of TM-2-PyP (220 mV), TM-4-PyP (60 mV), and TF_4TMAP (58 mV)(Supporting Information).[64] Consequently, the O−O bond cleavage in MnTDMImP is the slowest at 66 s^{-1} compared to MnTM-2-PyP (10^3 s^{-1}), MnTM-2-PyP, and MnTM-4-PyP ($> 10^4$ s^{-1}). Veeger has determined the O−O bond heterolysis rate for microperoxidase-8 to be 165 ± 8 for Fe^{III} and 145 ± 7 s^{-1} for Mn^{III}, respectively.[53] These values are comparable to our manganese porphyrins despite different high-valent metal species that are formed. The H_2O_2 heterolysis rate is generally facile in biological enzymes due to well positioned distal amino acid residues, for example, the lower limit for horseradish peroxidase was recently raised to be at least 10^4 s^{-1}.[65,66]

Overall Reaction pH Dependence. At low H_2O_2 concentrations, eq 2 can be written as:

$$k_{app} = \frac{k_{obs}}{[H_2O_2]} = k_2 K \qquad (3)$$

(56) Jones, P.; Dunford, H. B. *J. Inorg. Biochem.* **2005**, *99*, 2292–2298.
(57) Crestoni, M. E.; Fornarini, S.; Lanucara, F.; Warren, J. J.; Mayer, J. M. *J. Am. Chem. Soc.* **2010**, *132*, 4336–4343.
(58) Lahaye, D.; Groves, J. T. *J. Inorg. Biochem.* **2007**, *101*, 1786.
(59) Hewson, W. D.; Dunford, H. B. *Can. J. Chem.* **1975**, *53*, 1928–1932.
(60) Khan, K. K.; Mondal, M. S.; Mitra, S. *J. Chem. Soc., Dalton Trans.* **1998**, 533–536.
(61) Kaizer, J.; Costas, M.; Que, L. *Angew. Chem., Int. Ed.* **2003**, *42*, 3671–3673.
(62) Quinn, D. M. In *Isotopes Effects in Chemistry and Biology*; Kohen, A., Limbach, H. H., Eds.; CRC Press: Boca Raton, FL, 2006, p 995−1018.
(63) Kachadourian, R.; Johnson, C. A.; Min, E.; Spasojevic, I.; Day, B. J. *Biochem. Pharmacol.* **2004**, *67*, 77–85.
(64) Batinic-Haberle, I.; Spasojevic, I.; Hambright, P.; Benov, L.; Crumbliss, A. L.; Fridovich, I. *Inorg. Chem.* **1999**, *38*, 4011–4022.
(65) Shintaku, M.; Matsuura, K.; Yoshioka, S.; Takahashi, S.; Ishimori, K.; Morishima, I. *J. Biol. Chem.* **2005**, *280*, 40934–40938.
(66) Roth, J. P.; Cramer, C. J. *J. Am. Chem. Soc.* **2008**, *130*, 7802–7803.

Scheme 4

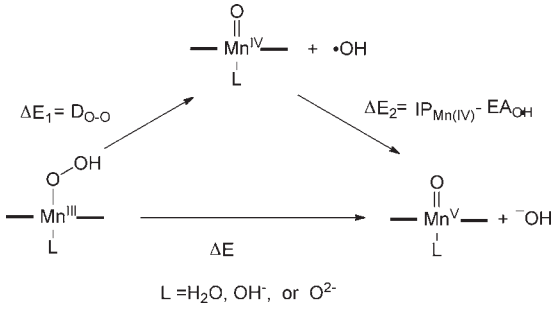

Since k_2 is pH independent, the pH dependence of the apparent overall reaction rate k_{app} is determined by K. The binding of H_2O_2 to Mn^{III}TDMImP generating **4** involves several acid−base equilibria. It appears that K increases with pH initially (Figure 4) since one or two protons are removed to form **4**. The lower reaction rate at higher pH can be ascribed to slow the ligand exchange rate for the dihydroxo Mn^{III} complex, which predominates at alkaline conditions.

This pH dependence is not unique to H_2O_2 as two other oxidants, HSO_5^- and *t*-BuOOH show similar pH dependence. This is to due to the fact that the oxidation mechanisms for HSO_5^-, *t*-BuOOH, and H_2O_2 are similar (Scheme 1). The peroxides are ligated to the manganese center first, followed by the O−O bond breaking. The pK_a values for HSO_5, H_2O_2, and t-BuOOH are comparable at 9.4, 11.75, and 12.25, respectively.[67,68]

Thermodynamics for O−O Bond Cleavage. The metal-mediated O−O bond heterolysis process has been analyzed by Shaik et al.[69] using a Hess cycle: a homolytic O−O cleavage followed by an electron transfer from Mn^{IV} to hydroxyl radical (Scheme 4). The overall energy change (ΔE) can be expressed as

$$\Delta E = D_{O-O} + IP_{Mn(IV)} - EA_{OH}. \quad (4)$$

The electron affinity of the hydroxyl radical (EA_{OH}.) is a constant, and the homolytic bond dissociation energy (D_{O-O}) depends to a small extent on the porphyrin ligand. For example, we have shown that the Mn^{IV}=O stretching frequency is the same for MnTM-2-PyP and MnTMP (711 and 712 cm^{-1}, respectively), indicative of very similar π-bonding.[70] Therefore, ΔE will be determined mostly by the ionization potential of the Mn^{IV} species ($IP_{Mn(IV)}$).

Ground states for quartet Mn^{IV} and singlet Mn^V have [d_{xy}(1), A_2u(2), A_1u(2), $d_\pi-\pi^*$(1), and $d_\pi-\pi^*$(1)] and [d_{xy}(1), A_2u(2), A_1u(2), $d_\pi-\pi^*$(1), and $d_\pi-\pi^*$(0)] electronic structures, respectively.[71,72] Ionization of the Mn^{IV} species involves ejection of an electron from $d_\pi-\pi^*$ orbital and pairing the other $d_\pi-\pi^*$ electron to the d_{xy} electron:

$$IP_{Mn(IV)} = -E(d_\pi - \pi*) + [E(d_\pi - \pi*) - E(d_{xy})] + C$$
$$= -E(d_{xy}) + C \quad (5)$$

The higher energy of the d_{xy} orbital results in a smaller $IP_{Mn(IV)}$ and thus a thermodynamically more favorable O−O bond cleavage. In the k_2 step transition state, the axial hydroxide ligand in the Mn^{III}(OH)(OOH) species is partially deprotonated with a negative charge accumulating on the axial oxygen atom. This electron redistribution would provide a larger field effect than the original OH^- due to the classic electron repulsion between d electrons and negative charges on ligands. The resulting electrostatic repulsion would be expected to increase the energy of the d_{xy} orbital, promote oxidation of the manganese, and facilitate the heterolytic breaking the distal O−O bond. Such a field effect can be quite significant; theoretical calculations by Shaik et al. have indicated that the negative charge on the thiolate proximal ligand in P450 provides a field effect of ~30 kcal/mol in an environment with a dielectric constant of 5.7.[69]

Our density functional theory (DFT) calculations showed that the d_{xy} orbital of MnTM-2-PyP is stabilized by 0.40 eV with respect to that of MnTM-4-PyP,[72] suggesting that the manganese center experiences an increased electron donation from the more electron-rich porphyrin ligand. This is a smaller effect compared to the strong axial push. Nonetheless, more electron-rich porphyrins were found to cleave the O−O bond much faster, even though the oxoMn^V species being formed is more reactive. We suggest that the reason the manganese(III)-hydroperoxo species of TDMImP can be observed but not with other water-soluble manganese porphyrins is that TDMImP is an unusually electron-deficient porphyrin ligand, as evidenced by the Mn^{II}/Mn^{III} redox couple and the unusually acidic aqua ligands (pK_a ~ 7).[58]

One can consider two extreme pathways for O−O bond cleavage in Mn^{III}(OH)(OOH): a "pull only" mechanism initiated by a direct protonation of the terminal oxygen in OOH^-, and a "push only" mechanism in which the axial OH^- is deprotonated first. In these two processes, a single "pull" or "push" may be sufficient to break the O−O bond. Indeed, Harris and Leow predicted protonation of the terminal oxygen in the Fe^{III}−OOH moiety leads to instantaneous O−O bond rupture,[73] and more modern computational approaches have also found a low barrier after protonation.[34] The results presented here indicate that an axial O^{2-} ligand provides a strong "push" rendering O−O bond breaking thermodynamically much more favorable. The lack of a pH dependence on the O−O bond cleavage step suggests the reaction proceeds through a concerted "push" and "pull" process in which the push and pull effects cooperate in lowering the activation enthalpy. The unfavorable entropy would derive from the necessary solvent reorganization around *both* axial ligands in the transition state.

(67) Meunier, B. *New J. Chem.* **1992**, *16*, 203–211.
(68) Curci, R.; Edwards, J. O. In *Catalytic Oxidations with Hydrogen Peroxide as oxidant*; Strukul, G., Ed.; Kluwer Acadmic Publishers: Dordrecht, The Netherlands, 1992, p 45−95.
(69) Ogliaro, F.; de Visser, S. P.; Shaik, S. *J. Inorg. Biochem.* **2002**, *91*, 554–567.
(70) Czernuszewicz, R. S.; Su, Y. O.; Stern, M. K.; Macor, K. A.; Kim, D.; Groves, J. T.; Spiro, T. G. *J. Am. Chem. Soc.* **1988**, *110*, 4158–4165.
(71) Ghosh, A.; Gonzalez, E. *Isr. J. Chem.* **2000**, *40*, 1–8.
(72) De Angelis, F.; Jin, N.; Car, R.; Groves, J. T. *Inorg. Chem.* **2006**, *45*, 4268–4276.
(73) Harris, D. L.; Loew, G. H. *J. Am. Chem. Soc.* **1998**, *120*, 8941–8948.

It is apparent that heme enzymes utilize such concerted "push−pull" effect to facilitate oxygen activation if needed. Peroxidases with an imidazole axial ligand have a particular hydrogen-bonding pattern in distal pockets that is adequate by itself to cleave O−O bond,[74] which represents the "pull" extreme. Positioning of the relavant functional groups by the protein scaffold would circumvent the entropy considerations described above. On the other hand, P450, chloroperoxidase, and NO synthase, which apparently have only a proton channel on the distal side of the heme, require a more electron-rich axial ligand (thiolate) to break the O−O bond efficiently, similar to the manganese porphyrins observed here.

We have demonstrated that O−Br bond-cleaving and -forming reactions are fast and *reversible* when mediated by similar manganese porphyrins.[45] While it is evident that O−O bond cleaving can be readily tuned by the porphyrin ligand and the reaction pH, we were not able to observe the corresponding O−O bond forming reactions. DioxoMn^{V} porphyrins, such as **2**, are relatively stable in alkaline conditions. Upon treatment with acid in the absence of reductants (such as Br^-), conversion to Mn^{III} species was always accompanied with some loss of the porphyrin chromophore (5−10%), suggesting that oxygen atom transfer to water, if achievable at all in our system, is much slower than that of Br^-. The difficulties of water oxidation can be readily understood if we apply the microscopic reversibility principle here: The reverse mechanism (Scheme 3) suggests simultaneously adding a proton and a hydroxide ion to a dioxo Mn^{V} porphyrin, indicating a very high-entropy barrier. Furthermore, Br^- oxidation is greatly accelerated by lowering the pH.[45] In the water oxidation reaction, however, higher proton concentrations would always result in lower hydroxide concentration, rendering pH adjustment ineffective. Interestingly, the revesible conversion of an oxomanganese(V) corrole to a manganese peroxo complex has very recently been reported.[42] This was a nonaqueous system where the arguments above may not apply. In the photosystem II, nature has apparently lowered the entropy barrier with carefully orchestrated hydrogen-bonding networks and, perhaps, overcomes the aforementioned paradox by using a metal ion (Mn^{2+} or Ca^{2+}) coordinated hydroxide attack on a high-valent oxo manganese cluster.[75]

Conclusions

We have spectroscopically observed and kinetically characterized an intermediate Mn^{III}(OH)(OOH)TDMImP complex analogous to the compound 0 of heme proteins. The O−O bond cleavage has been shown to occur via a concerted "push−pull" mechanism. In the transition state, the axial OH^- is partially deprotonated ("push") as it is transformed into an oxo ligand, while the terminal oxygen in OOH^- is partially protonated ("pull") as it forms a water molecule. A large, negative entropy was observed for this step largely due to the simultaneous solvation of the proton and the hydroxide anion. Consequently, the O−O bond heterolysis is pH independent even though several acid−base equilibria exist before this step. The demonstration of a functional "push−pull" mechanism with a very small activation enthalpy in this small molecule model porphyrin system may provide pointers for future advances in transition-metal mediated O−O bond-cleaving and -forming reactions.

Experimental Section

Materials. Manganese(III)-5,10,15,20-tetrakis-(1,3-dimethylimidazolium-2-yl)porphyrin chloride (Mn^{III}TDMImP), manganese(III)-5,10,15,20-tetrakis(*N*-methylpyridinium-4-yl)porphyrin chloride, (Mn^{III}TM-4-PyP), manganese(III)-5,10,15,20-tetrakis(*N*-methylpyridinium-2-yl)porphyrin chloride, (Mn^{III}TM-2-PyP), and manganese(III)-5,10,15,20-tetrakis(2,3,5,6-tetrafluoro-*N*,*N*,*N*-trimethyl-4-aniliniumyl)porphyrin trifluoromethanesulfonate (Mn^{III}TF$_4$TMAP) were either purchased from Mid-Century (Posen, IL) or synthesized according to published procedures.[76−78] These compounds were further purified by a double-precipitation method,[77] except that Mn^{III}TF$_4$TMAP was used as received. Water used in all experiments was distilled and deionized by a Milli-Q system (Millipore). Hydrogen peroxide (30%), *t*-butyl hydroperoxide (70%), cumene hydroperoxide (88%), and oxone (Potassium peroxomonosulfate, 90%) were obtained from Aldrich, and their purity was measured iodometrically. All diluted solutions of these oxidants were freshly prepared before kinetic studies. Buffer solutions were prepared by mixing appropriate amounts of acid or base species of Tris or phosphate (pH = 7.5−8.5), borate (pH = 8.5−9.5), carbonate (pH = 9.5−11), phosphate (pH = 11−12), and NaOH (pH = 12+) in water and adjusted by either HCl or NaOH solutions. Deuterated borate buffer was prepared using anhydrous sodium tetraborate and $DClO_4$, p*D* value was determined by adding 0.4 to pH meter readings. In single-wavelength kinetic studies, ionic strength was maintained by 0.1 M sodium perchlorate (twice recrystallized in deionized water). Actual pH was measured after the reaction by an Accumet AB15 pH meter (Fisher Scientific) using a combined glass electrode and calibrated by standard (pH = 7.00, 10.00) and FIXANAL (Aldrich pH = 13.00) calibration solutions at 25 °C.

Stopped-Flow Spectroscopy. Stopped-flow experiments were performed on a Hi-Tech SF-61 DX2 spectrophotometer using a 1 cm path length with a mixing time of approximately 1.5 ms. Temperature was regulated with a thermostat water bath, all kinetic data were measured in 25.0 ± 0.2 °C unless otherwise noted. Kinetic and thermodynamic constants are presented with 95% confidence in the format of $x \pm 2\sigma$. Indicated concentrations in the Results Section are the final concentrations after mixing. Typically, manganese porphyrins (2−20 μM) in a buffer solution with 0.1 M $NaClO_4$ were fast mixed with a freshly prepared unbuffered oxidant solution (to decrease auto decomposition) with 0.1 M $NaClO_4$. Measurements were performed three to five independent times under pseudofirst-order conditions with at least a 10-fold excess of oxidants with respect to manganese porphyrins. Time-resolved UV−vis spectra were recorded in diode array mode with a spectral resolution of about 1 nm. Spectrum of the intermediate was deconvoluted by SPECFIT/32 global analysis system from Bio-Logic. The extremes, corresponding to Mn^{III} and Mn^{V}, were set as fixed, and a two-consecutive reaction mechanism was applied. Single-wavelength kinetic profiles were collected in photomultiplier mode by following the formation of Mn^{V}TDMImP (426 nm), Mn^{V}TM-2-PyP (432 nm), Mn^{V}TM-4-PyP (441 nm), and Mn^{V}TF$_4$TMAP (426 nm) or the disappearance of Mn^{III}TDMImP (446 or 435 nm depending on pH), and data were processed using Hi-Tech KinetAsyst 3 software. At low oxidant concentrations, k_{app} was calculated from a linear fit of k_{obs} vs oxidant concentration.

(74) Poulos, T. L. *J. Biol. Inorg. Chem.* **1996**, *1*, 356–359.
(75) Brudvig, G. W. *Philos. Trans. R. Soc., B* **2008**, *363*, 1211–1218.
(76) Tjahjono, D. H.; Akutsu, T.; Yoshioka, N.; Inoue, H. *Biochim. Biophys. Acta* **1999**, *1472*, 333–343.
(77) Batinic-Haberle, I.; Benov, L.; Spasojevic, I.; Fridovich, I. *J. Biol. Chem.* **1998**, *273*, 24521–24528.
(78) La, T.; Richards, R.; Miskelly, G. M. *Inorg. Chem.* **1994**, *33*, 3159–3163.

General Instrumentation. UV−vis spectral measurements were carried out on a Hewlett-Packard 8453 diode-array spectrophotometer using 1 cm path standard quartz cells. NMR spectra were recorded on a 500 MHz Varian spectrometer. Electron paramagnetic resonance (EPR) experiments were performed on a Bruker Elexys 580 X-band CW-EPR system with dual mode cavity at 5 K.

Acknowledgment. Support of this research by the National Science Foundation (CHE 0316301) is gratefully acknowledged.

Supporting Information Available: UV−vis, NMR, EPR spectra, Eyring plot, and KSIE measurement kinetic data. This material is available free of charge via the Internet at http://pubs.acs.org